This article has been accepted for publication in a future issue of this journal, but has not been fully edited. Content may change prior to final publication. Citation information: DOI 10.1109/TIA.2018.2798593, IEEE Transactions on Industry Applications

Performance Improvement of Three-Level Five-Phase Inverter Fed DTC Controlled Five-Phase Induction Motor during Low-Speed Operation

Yogesh N. Tatte, Mohan V. Aware, Jay Pandit and Ronak Nemade

***Abstract*— In this paper, the Direct Torque Control (DTC) for three-level five-phase inverter fed five-phase induction motor is proposed to improve the low speed performance. The classical DTC scheme (DTC-I) is modified in order to minimize the demagnetization effect during low speed operation. According to modification, the voltage vector space plane is divided into twenty sectors, each of sector 18º. For odd number of sectors, ±36º displaced intermediate voltage vectors and for even number of sectors, ±36º displaced main voltage vectors are selected instead of classic ±72º displaced voltage vectors. The zero voltage vectors are omitted in the proposed DTC scheme (DTC-II) for the low speed operation. The DTC-II scheme reduces the demagnetization effect during low speed region at the cost of increase in torque ripple due to avoiding zero voltage vectors. As the speed ramps up the ±72º displaced voltage vectors are selected through seven-level torque comparator and are divided in ten sectors. Therefore in the medium and the higher speed region the torque ripple are reduced by using seven-level torque comparator. Simulation and experimental results are presented in order to validate the DTC-II method.**

Keywords*— *Direct Torque Control; three-level five-phase Inverter; low-speed operation; demagnetization effect; torque ripple.

I. INTRODUCTION

The direct torque control technique is invented in 1986 by Takahashi and Noguchi for three-phase induction motor [1]. The advent in semiconductor technology makes it possible to extend the basic switching table DTC scheme for the three-phase induction motor [1] to the five-phase induction motor [2]. The five-phase induction motor with DTC control technique is then modified several times to improve its performance in context of stator current distortion, torque ripple, low speed region stator flux increment, etc. [3]-[6].

The classical two-level five-phase DTC scheme aims sluggish torque response and demagnetization of the stator flux during low speed operation. Establishment of stator flux is necessary in direct torque controlled induction motor. However, maintaining the stator flux constant at rated value is difficult during the low speed operation of the motor, because the voltage drop on the stator resistance becomes comparable to the input stator voltage. In case of three-phase induction motor drive, the operation of the machine in the low speed region is improved by various techniques presented in [7]-[9]. Gao *et al*. [5] introduced a technique to improve the demagnetization effect during low speed operation of the five phase induction motor, wherein the classical DTC algorithm has been modified so that ±72º displaced voltage vectors are replaced with ± 36º displaced voltage vectors. These ± 36º displaced voltage vectors have reduced the flux demagnetization during low speed operation of the five-phase induction motor fed by two-level five-phase inverter. New modification in the voltage vector selection is proposed in [6], wherein the demagnetization in the stator flux is reduced to improve the low speed performance of the five-phase induction motor.

The three-level five-phase Space Vector Pulse Width Modulation technique is proposed in [10], [11], where switching strategy utilizes 113 candidate voltage vectors to develop the desired voltage reference out of available $3^5 = 243$ voltage vectors. Optimized five vectors modulation technique is used to develop the reference voltage, where there are ten switching events during each modulation cycle. This space vector modulation technique increases space voltage vectors from 32 in two-level to 113 in three-level. As the numbers of voltage vectors are increased, freedom to use them for reducing the demagnetization effect can be enhanced. The literatures presented in last two decades indicated that five phase induction motor when controlled by classical DTC technique and fed from two-level inverter suffers from low speed region demagnetization. If five-phase induction motor is controlled by classical DTC technique and fed from three-level five-phase inverter, the freedom of selecting more accurate voltage vectors is increased as compared to two-level five-phase inverter [12], [13], [15], [16], [18]. Therefore the problem of demagnetization during low speed operation can be resolved more efficiently by utilizing the freedom of selecting more accurate voltage vectors in the three-level five-phase inverter.

In this paper, the low speed operation of the DTC controlled five-phase induction motor fed by three-level five-phase inverter is investigated and the modification in the classical DTC scheme is proposed to improve its performance. According to modification, 60 voltage vectors including main and intermediate and excluding zero voltage vectors are used out of 243 available voltage vectors which are divided into 20 sectors each of width 18º in the low speed region. The DTC-II scheme achieves reduction in demagnetization under low speed operation at the expense of slight increase in torque ripple. Therefore once the speed enters into normal speed region (above 20% of rated speed) voltage vector selection scheme changes and only main 42 voltage vectors are employed through seven-level torque comparator to reduce the torque ripple. In the proposed algorithm, virtual voltage vectors are formed which eliminates the *x-y* stator flux. The four-level hysteresis torque comparator is used for low speed

operation to omit the utilization of zero voltage vectors because it causes drooping of the flux. In order to bring the better responses during the low speed operation, an adaptive observer is also employed [7]. The estimation of the stator flux, the stator resistance and the rotor speed are done by using an adaptive full-order observer. The simulation and experimental results validates the DTC-II scheme.

This paper is organized as follows. Section II introduces distribution of voltage vectors among DTC-I and DTC-II methods. In section III, improvement in performance during low speed operation is presented. Section IV details the selection of the voltage vectors in the control algorithms. Simulation results are presented in section V and experimental in section VI. Section VII deals with the conclusions from the presented work.

II. Distribution of Voltage Vectors Among DTC-I and DTC-II Methods

The schematic of three-level five-phase inverter which is extended from basic three-phase three-level inverter NPC inverter is shown in fig. 1(a) [17]. The three-level five-phase inverter has 243 voltage vectors consisting of 240 active and 3 zero. The switch function of these voltage vectors is represented as $S = [S_A\ S_B\ S_C\ S_D\ S_E]^T$, where $S_i = 2$ or 0 or 1, state 2 represents turning ON of upper two switches, state 0 represents turning ON of lower two switches and state 1 represents turning ON of middle two switches, whereas remaining switches for the particular state remains OFF. The state variable form of machine equation in terms of stator and rotor flux in stationary reference frame can be expressed in matrix form.

$$\begin{bmatrix} \frac{d\lambda_s}{dt} \\ \frac{d\lambda_r}{dt} \end{bmatrix} = \begin{bmatrix} -\frac{r_s}{\sigma L_s} & \frac{r_s L_m}{\sigma L_s L_r} \\ \frac{r_r L_m}{\sigma L_s L_r} & j\omega_m - \frac{r_r}{\sigma L_r} \end{bmatrix} \begin{bmatrix} \lambda_s \\ \lambda_r \end{bmatrix} + \begin{bmatrix} 1 \\ 0 \end{bmatrix} V_s \qquad (1)$$

where, L_m is the mutual inductance, L_s is the stator inductance, L_r is the rotor inductance, leakage coefficient, $\sigma = 1 - \frac{L_m^2}{L_s L_r}$, λ_s is stator flux complex vector representing d and q axis with $\lambda_s = \lambda_{ds} + j\lambda_{qs}$., λ_r is rotor flux complex vector representing d and q axis with $\lambda_r = \lambda_{dr} + j\lambda_{qr}$, V_s is stator voltage complex vector representing d and q axis with $V_s = V_{ds} + jV_{qs}$, r_s represents the stator resistance, r_r represents the rotor resistance and ω_m is the motor angular velocity. The electromagnetic torque can be written as

$$T_e = \frac{5}{2} P \frac{L_m}{\sigma L_s L_r} \mathrm{Im}[\lambda_s . \lambda_r^*] \qquad (2)$$

where, P is the number of pole pairs and * denotes the complex conjugate. The voltage vectors are selected in order to control the torque, while maintaining the stator flux equals to its reference rated value.

Out of 113 candidate voltage vectors in the three-level five-phase inverter, 72 voltage vectors are used in designing DTC-I and DTC-II methods. Fig. 1(b) and fig. 1(c) shows the distribution of all 72 voltage vectors in d-q space plane and x-y space plane respectively. These voltage vectors are mainly classified according to their location into three groups, i.e. main, intermediate and zero voltage vectors. The voltage vectors numbered from V_1-V_{40} are main voltage vectors, V_{41}-V_{70} are intermediate voltage vectors and V_0 and V_{71} are zero voltage vectors. Out of these 72 voltage vectors, main 30 (V_1-V_{30}), intermediate 30 (V_{41}-V_{70}) and 2 zero voltage vectors, in all 62 voltage vectors are employed in DTC-I scheme. This scheme has five-level torque comparator working throughout the complete speed range. However, in DTC-II method, 60 voltage vectors (V_1-V_{30}, V_{41}-V_{70}) are employed through four level torque comparator and divided into twenty sectors for low speed operation. For normal speed operation main V_1-V_{40} and two zero voltage vectors (V_0 and V_{71}), in all 42 voltage vectors are employed through seven-level torque comparator and divided into ten sectors each of width 36°.

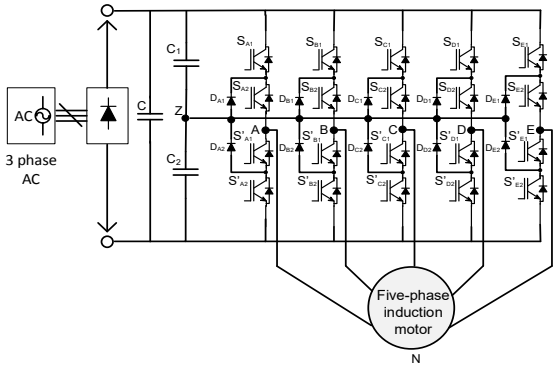

(a)

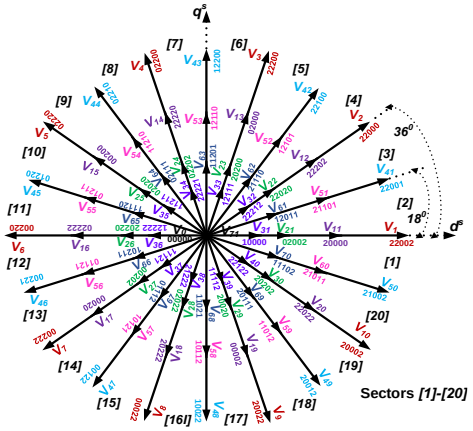

(b)

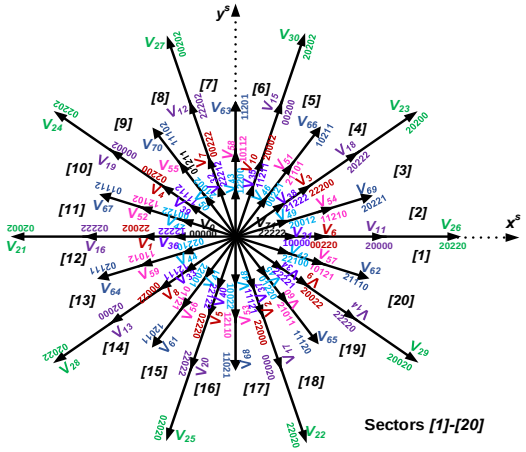

(c)

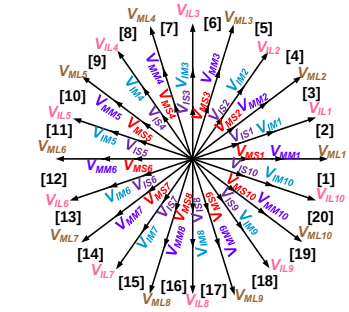

(d)

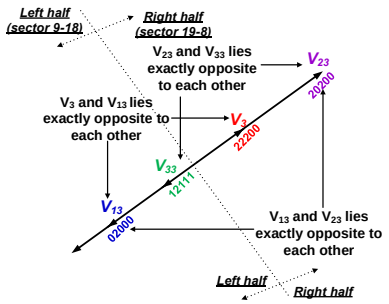

(e)

Fig. 1 Three-level five-phase inverter, (a) schematic, (b) voltage vectors mapped in *d-q* plane, (c) voltage vectors mapped in *x-y* plane, (d) virtual voltage vectors mapped in *d-q* plane and (e) oppositely located voltage vectors.

While designing both the DTC-I and DTC-II schemes for the five-phase induction motor, the magnitude of *x-y* stator flux should also be considered. The *x-y* space plane also exists in the five-phase motor which is decoupled and orthogonal to *d-q* space plane. There is no coupling of *x-y* component with the rotor circuit. The electromagnetic torque is produced by *d-q* component only and the *x-y* component simply causes losses in the machine. So it becomes necessary to eliminate the magnitude of *x-y* stator flux components. In order to eliminate the *x-y* stator flux, the virtual voltage vectors are formed. The virtual voltage vectors group of main large voltage vectors V_{MLX} consists of actual voltage vectors V_1-V_{10} and V_{11}-V_{20}, main medium virtual voltage vectors V_{MMX} consists of V_{11}-V_{20} and V_{21}-V_{30} and main small virtual V_{MSX} consists of actual voltage vectors V_{21}-V_{30} and V_{31}-V_{40}. The virtual group of intermediate large voltage vectors V_{ILX} consists of actual voltage vectors V_{41}-V_{50} and V_{51}-V_{60} and intermediate small virtual voltage vectors V_{ISX} consists of actual voltage vectors V_{51}-V_{60} and V_{61}-V_{70}, where X=1-10. In DTC-I, 10 V_{MLX}, 10 V_{MMX}, 10 V_{ILX}, 10 V_{ISX} and two zero voltage vectors are employed. In DTC-II scheme 10 V_{MLX}, 10 V_{MMX}, 10 V_{ILX} and 10 V_{ISX} are employed for low speed region and all the main virtual voltage vectors and zero voltage vectors except intermediate are employed for normal speed operation.

All the virtual voltage vectors which are employed in both the DTC schemes are depicted in fig. 1(d). Once the virtual voltage vector is selected, the actual voltage vector is selected depending upon the location of *x-y* stator flux in order to eliminate the *x-y* stator flux. The voltage vectors V_1-V_{10} are located exactly opposite to voltage vectors V_{11}-V_{20}, similarly V_{11}-V_{20} are located exactly opposite to V_{21}-V_{30} and V_{21}-V_{30} are located exactly opposite to V_{31}-V_{40}. Similarly intermediate voltage vectors are also located opposite to each other. The selection of actual voltage vector will be done by the following procedure. Consider the example of main large virtual voltage vector V_{ML3} as shown in fig. 1(e),

- Check the location of *x-y* stator flux ($\alpha = \tan^{-1}(\lambda_{sy}/\lambda_{sx})$ in fig. 6), where λ_{sx} and λ_{sy} are *x-y* stator flux.
- If *x-y* stator flux lies in sector (9-18), V_3 will be selected.
- If *x-y* stator flux lies in sector (19-8), V_{13} will be selected.

Similarly actual voltage vectors from remaining virtual voltage vectors will be selected. The selection of opposite voltage vectors to the location of *x-y* stator flux eliminates the *x-y* stator flux [5].

III. Improvement in Performance During Low Speed Operation

In DTC-I, the classic selection of voltage vectors causes drooping of the stator flux during low speed operation. The drooping of stator flux has been overcome by the DTC-II strategy. According to modification, ±72° displaced voltage vectors and the zero voltage vectors are replaced by ±36° displaced main and the intermediate voltage vectors. The demagnetization effect, when the stator flux lies in even sector is shown in fig. 2(a). It is seen that the stator flux λ_s^* is decreased in the region near the sector to sector boundary by the utilization of 72° displaced voltage vector V_{ML3} which is selected by the DTC-I strategy ($\lambda_{s1}<\lambda_s^*$). In DTC-II method, the 72° displaced voltage vector is replaced by 36° displaced voltage vector in order to increase the value of stator flux ($\lambda_{s1}>\lambda_s^*$). Therefore by applying 36° displaced voltage vector V_{ML2}, the stator flux is increased as shown in fig. 2(b).

In odd sectors, the intermediate voltage vectors are used. The demagnetization during low speed operation when the stator flux lies in odd sector is shown in fig. 2(c). Fig. 2(c) shows the stator flux λ_s^* decreasing in the region near the sector to sector boundary by the utilization of 72° displaced voltage vector V_{IL2} ($\lambda_{s1}<\lambda_s^*$) in DTC-I method. In DTC-II method, this voltage vector is replaced by 36° displaced voltage vector V_{IL1}. Fig. 2(d) shows that the stator flux is increased by the utilization of intermediate voltage vector V_{IL1} ($\lambda_{s1}> \lambda_s^*$). The selection of zero voltage vectors droops the stator flux, hence they are omitted from the DTC-II strategy [15]. The zero voltage vectors are applied once the speed ramps up and enter into the normal speed range. Under normal speed operation, the seven-level torque comparator is implemented in DTC-II method to reduce the torque ripple.

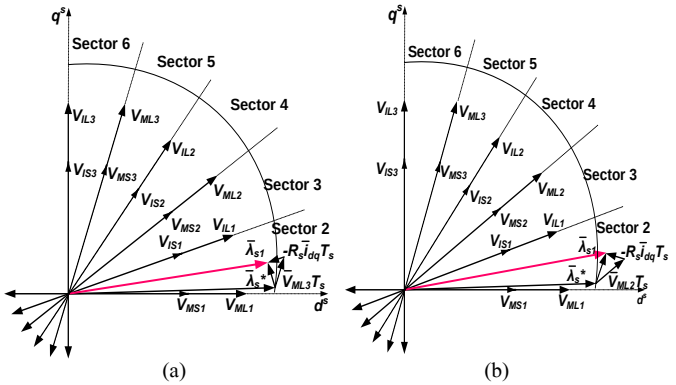

(a) (b)

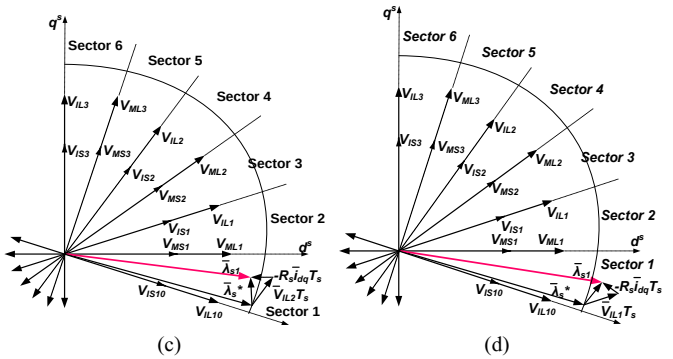

Fig. 2 Demagnetization effect, DTC-I (left) and DTC-II (right), even sectors (a, b) and odd sectors (c, d).

When the DTC-II scheme is compared with the earlier proposed DTC scheme [5], it is observed that the final stator flux decreases ($\lambda_{s3}<\lambda_{s1}^*$) according to [5] as shown in fig. 3(a). However, in DTC-II scheme the stator flux increases ($\lambda_{s3}>\lambda_{s1}^*$) as shown in fig. 3(b). The main large virtual voltage vectors have the dc-bus length of $(0.647+0.4)V_{dc}/2=0.5235V_{dc}$ and intermediate large virtual voltage vectors have the dc-bus length of $(0.615+0.380)V_{dc}/2=0.4975V_{dc}$ [10]-[14]. The ratio of radial component of V_{IL1}/V_{ML2} which increases the stator flux = $(0.4975V_{dc}*\cos 18)/(0.5235V_{dc}*\cos 36)$ = 1.1171. Therefore in DTC-II scheme the stator flux gain is 11.71% more than the scheme proposed in [5].

Figs. 4(a) and 4(b) show the representation and operation of the torque comparator used in low speed region and normal speed region respectively in the DTC-II scheme.

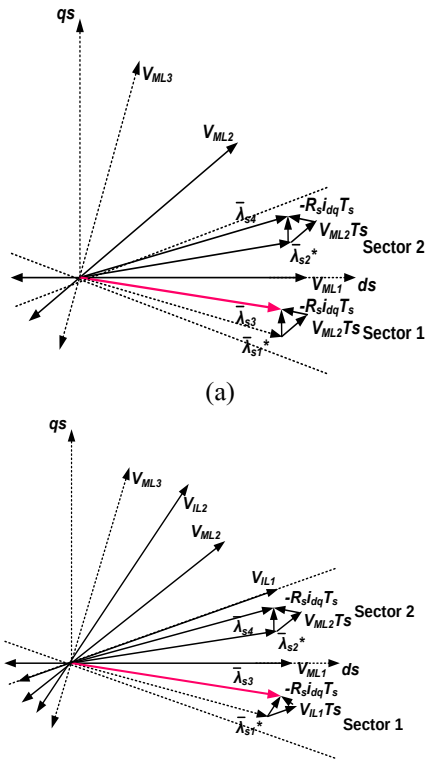

Fig. 3 Demagnetization effect comparison, (a) DTC strategy proposed in [5] and (b) DTC-II.

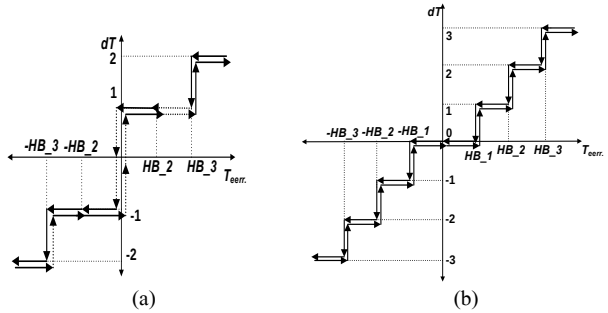

Fig. 4 Representation of different torque comparators, (a) four-level torque comparator (low speed region) and (b) seven-level torque comparator (normal speed region).

IV. Selection of Voltage Vector

The operational conditions of the four-level torque and two-level flux comparators for low speed operation are as follows:

$\lambda_s<\lambda_s^*$ $d\lambda=1$ (3)

$\lambda_s^*<\lambda_s$ $d\lambda=0$ (4)

$T_e^*-T_e \geq$ *Hysteresis band* $dT=2$ (5)

Hysteresis band $>T_e^*-T_e\geq 0$ $dT=1$ (6)

$T_e^*-T_e\leq$ *-(Hysteresis band)* $dT=-2$ (7)

-(Hysteresis band) $<T_e^*-T_e\leq 0$ $dT=-1$ (8)

Table I (A) depicts the selection of suitable virtual voltage vector group according to the output from flux comparator, torque comparators and the location of *d-q* stator flux for the low speed operation. Table I (B) selects the actual voltage vector based on the output from the table I (A) and the location of *x-y* stator flux. For example when the *d-q* stator flux lies in the first sector, if both torque and flux are required to increase ($dT=2$ and $d\lambda=1$), the intermediate large virtual voltage vector V_{IL1} is selected by table I (A), dT=2 represents the requirement of fast increment in actual torque, whereas dT=1 represents the requirement of slow increment in actual torque. If V_{IL1} is selected by table I (A) and if *x-y* stator flux lies in third sector, the actual voltage vector V_{41} is selected by table I (B). V_{41} is selected when the *x-y* stator flux lies from sector no. 20 to 9. In case of selection of main voltage vector, for example, if *d-q* stator flux lies in sector no. 12, if both the torque and the flux are required to decrease ($dT=-1$ and $d\lambda=0$), the virtual main small voltage vector V_{MM3} is selected by table I (A). By selecting V_{MM3}, either V_{13} or V_{23} will be selected by table I (B) depending upon the location of *x-y* stator flux. Depending upon the rotor speed, the operation of the torque controller selects. For low speed operation, four-level torque controller will be selected and in the normal speed region (above 20% of the rated speed), 72° displaced voltage vectors are selected through seven-level torque comparator which is mentioned in [16]. The voltage vector selection procedure of DTC-I scheme is mentioned in [5], [13].

The five phase induction motor is driven by three-level five-phase inverter and is controlled by DTC algorithm as shown in fig. 5. In order to improve the performance of machine in the low speed region a high performance speed sensorless DTC algorithm is implemented. The estimation of the stator flux, the stator resistance and the rotor speed are done by using an adaptive full-order observer [7].

TABLE I (A) Selection of virtual voltage vectors for low speed operation.

$d\lambda$	dT	Sector identification from angle ϕ=tan^{-1} (λ_{sq}/ λ_{sd})), for example if $-18^0<\phi<=0^0$, sector=1																			
		1	2	3	4	5	6	7	8	9	10	11	12	13	14	15	16	17	18	19	20
0	2	V_{IL3}	V_{ML4}	V_{IL4}	V_{ML5}	V_{IL5}	V_{ML6}	V_{IL6}	V_{ML7}	V_{IL7}	V_{ML8}	V_{IL8}	V_{ML9}	V_{IL9}	V_{ML10}	V_{IL10}	V_{ML1}	V_{IL1}	V_{ML2}	V_{IL2}	V_{ML3}
	1	V_{IS3}	V_{MM4}	V_{IS4}	V_{MM5}	V_{IS5}	V_{MM6}	V_{IS6}	V_{MM7}	V_{IS7}	V_{MM8}	V_{IS8}	V_{MM9}	V_{IS9}	V_{MM10}	V_{IS10}	V_{MM1}	V_{IS1}	V_{MM2}	V_{IS2}	V_{MM3}
	-1	V_{IS7}	V_{MM8}	V_{IS8}	V_{MM9}	V_{IS9}	V_{MM10}	V_{IS10}	V_{MM1}	V_{IS1}	V_{MM2}	V_{IS2}	V_{MM3}	V_{IS3}	V_{MM4}	V_{IS4}	V_{MM5}	V_{IS5}	V_{MM6}	V_{IS6}	V_{MM7}
	-2	V_{IL7}	V_{ML8}	V_{IL8}	V_{ML9}	V_{IL9}	V_{ML10}	V_{IL10}	V_{ML1}	V_{IL1}	V_{ML2}	V_{IL2}	V_{ML3}	V_{IL3}	V_{ML4}	V_{IL4}	V_{ML5}	V_{IL5}	V_{ML6}	V_{IL6}	V_{ML7}
1	2	V_{IL1}	V_{ML2}	V_{IL2}	V_{ML3}	V_{IL3}	V_{ML4}	V_{IL4}	V_{ML5}	V_{IL5}	V_{ML6}	V_{IL6}	V_{ML7}	V_{IL7}	V_{ML8}	V_{IL8}	V_{ML9}	V_{IL9}	V_{ML10}	V_{IL10}	V_{ML1}
	1	V_{IS1}	V_{MM2}	V_{IS2}	V_{MM3}	V_{IS3}	V_{MM4}	V_{IL4}	V_{MM5}	V_{IL5}	V_{MM6}	V_{IS6}	V_{MM7}	V_{IS7}	V_{MM8}	V_{IS8}	V_{MM9}	V_{IS9}	V_{MM10}	V_{IS10}	V_{MM1}
	-1	V_{IS9}	V_{ML10}	V_{IS10}	V_{ML1}	V_{IS1}	V_{ML2}	V_{IS2}	V_{ML3}	V_{IS3}	V_{ML4}	V_{IS4}	V_{ML5}	V_{IS5}	V_{ML6}	V_{IS6}	V_{ML7}	V_{IS7}	V_{ML8}	V_{IS8}	V_{ML9}
	-2	V_{IL9}	V_{MM10}	V_{IL10}	V_{MM1}	V_{IL1}	V_{MM2}	V_{IL2}	V_{MM3}	V_{IL3}	V_{MM4}	V_{IL4}	V_{MM5}	V_{IL5}	V_{MM6}	V_{IL6}	V_{MM7}	V_{IL7}	V_{MM8}	V_{IL8}	V_{MM9}

TABLE I (B) Selection of actual voltage vectors

V_{ML}	V_{ML1}	V_{ML2}	V_{ML3}	V_{ML4}	V_{ML5}	V_{ML6}	V_{ML7}	V_{ML8}	V_{ML9}	V_{ML10}
	V_1 (17-6)	V_2 (3-12)	V_3 (9-18)	V_4 (15-4)	V_5 (1-10)	V_6 (7-16)	V_7 (13-2)	V_8 (19-8)	V_9 (5-14)	V_{10} (11-20)
	V_{11} (7-16)	V_{12} (13-2)	V_{13} (19-10)	V_{14} (5-14)	V_{15} (11-20)	V_{16} (17-6)	V_{17} (3-12)	V_{18} (9-18)	V_{19} (15-4)	V_{20} (1-10)
V_{MM}	V_{MM1}	V_{MM2}	V_{MM3}	V_{MM4}	V_{MM5}	V_{MM6}	V_{MM7}	V_{MM8}	V_{MM9}	V_{MM10}
	V_{21} (17-6)	V_{22} (3-12)	V_{23} (9-18)	V_{24} (15-4)	V_{25} (1-10)	V_{26} (7-16)	V_{27} (13-2)	V_{28} (19-8)	V_{29} (5-14)	V_{30} (11-20)
	V_{11} (7-16)	V_{12} (13-2)	V_{13} (19-8)	V_{14} (5-14)	V_{15} (11-20)	V_{16} (17-6)	V_{17} (3-12)	V_{18} (9-18)	V_{19} (15-4)	V_{20} (1-10)
V_{MS}	V_{MS1}	V_{MS2}	V_{MS3}	V_{MS4}	V_{MS5}	V_{MS6}	V_{MS7}	V_{MS8}	V_{MS9}	V_{MS10}
	V_{21} (17-6)	V_{22} (3-12)	V_{23} (9-18)	V_{24} (15-4)	V_{25} (1-10)	V_{26} (7-16)	V_{27} (13-2)	V_{28} (19-8)	V_{29} (5-14)	V_{30} (11-20)
	V_{31} (7-16)	V_{32} (13-2)	V_{33} (19-8)	V_{34} (5-14)	V_{35} (11-20)	V_{36} (17-6)	V_{37} (3-12)	V_{38} (9-18)	V_{39} (15-4)	V_{40} (1-10)
V_{IL}	V_{IL1}	V_{IL2}	V_{IL3}	V_{IL4}	V_{IL5}	V_{IL6}	V_{IL7}	V_{IL8}	V_{IL9}	V_{IL10}
	V_{41} (20-9)	V_{42} (6-15)	V_{43} (12-1)	V_{44} (18-7)	V_{45} (4-13)	V_{46} (10-19)	V_{47} (16-5)	V_{48} (2-11)	V_{49} (8-17)	V_{50} (14-3)
	V_{51} (10-19)	V_{52} (16-5)	V_{53} (2-11)	V_{54} (8-17)	V_{55} (14-3)	V_{56} (20-9)	V_{57} (6-15)	V_{58} (12-1)	V_{59} (18-7)	V_{60} (4-13)
V_{IS}	V_{IS1}	V_{IS2}	V_{IS3}	V_{IS4}	V_{IS5}	V_{IS6}	V_{IS7}	V_{IS8}	V_{IS9}	V_{IS10}
	V_{61} (20-9)	V_{62} (6-15)	V_{63} (12-1)	V_{64} (18-7)	V_{65} (4-13)	V_{66} (10-19)	V_{67} (16-5)	V_{68} (2-11)	V_{69} (8-17)	V_{70} (14-3)
	V_{51} (10-19)	V_{52} (16-5)	V_{53} (2-11)	V_{54} (8-17)	V_{55} (14-3)	V_{56} (20-9)	V_{57} (6-15)	V_{58} (12-1)	V_{59} (18-7)	V_{60} (4-13)

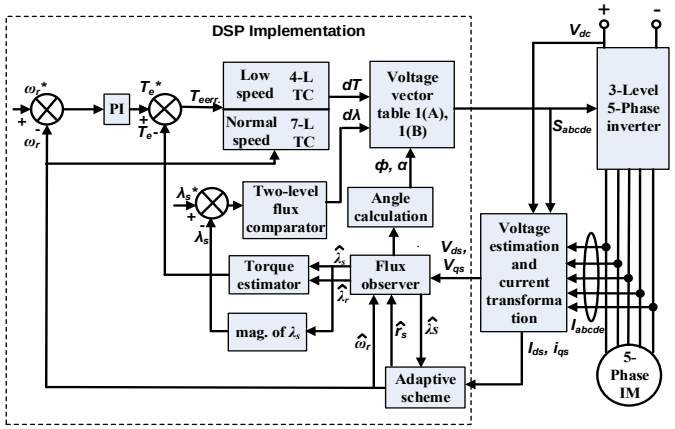

Fig. 5 Control block diagram of DTC-II scheme.

$$\frac{d}{dt}\hat{x} = \hat{A}\hat{x} + BV_s + G(\hat{i}_s - i_s) \tag{9}$$

$$\hat{x} = \begin{bmatrix} \hat{i}_{ds} & \hat{i}_{qs} & \hat{\lambda}_{dr} & \hat{\lambda}_{qr} \end{bmatrix}^T \tag{10}$$

$$\hat{\omega}_r = k_p(e_{ids}\hat{\lambda}_{qr} - e_{iqs}\hat{\lambda}_{dr} + k_i\int(e_{ids}\hat{\lambda}_{qr} - e_{iqs}\hat{\lambda}_{dr})dt \tag{11}$$

$$\frac{d}{dt}\hat{r}_s = -k_1(e_{ids}\hat{i}_{ds} + e_{iqs}\hat{i}_{qs}) \tag{12}$$

$$e_{ids} = i_{ds} - \hat{i}_{ds}, \quad e_{iqs} = i_{qs} - \hat{i}_{qs} \tag{13}$$

where i_{ds} and i_{qs} represent d and q axis stator current, $\hat{i}_{ds}$ and $\hat{i}_{qs}$ represent estimated current values and the constants are k_p= 2, k_i=6 and k_1=1.

V. Experimental Results

Fig. 6 shows laboratory prototype of both the DTC-I and DTC-II methods which consists of five-phase induction motor connected to dc machine, TMS320F28377S floating point DSP, an IGBT inverter, three-phase uncontrolled rectifier, and sensor circuit consisting of four LEM LA 25-P current sensors and LEM LV 20-P voltage sensor. HEDS-5645-I13 encoder is used for speed sensing. A small around 1 Hp cage type

symmetrical five-phase induction motor is taken. It has $r_s = 0.8$ Ω, $r_r = 0.6$ Ω, $L_{ls} = 2.6$ mH, $L_{lr} = 2.6$ mH, $L_m = 151$mH, rotor inertia (J) = 0.047kg-m^2 and $P = 2$, V_{dc} =400V. The rated torque, flux and speed are 6Nm, 0.54Wb and 1500rpm respectively. The Experimental results are presented in order to validate the DTC-II method. The sampling frequency set for both the schemes is 22 kHz. Figs. 7 and 8 show the results of dynamic operation of DTC-I and DTC-II methods respectively. It is seen that in DTC-I, the selection of voltage vectors cannot maintain the *d-q* stator flux at rated value, however in DTC-II the selection of voltage vectors maintains the *d-q* stator flux at rated value throughout the operation. It is also observed that omitting zero voltage vectors in DTC-II scheme increases torque ripple compared to DTC-I scheme. In both the presented DTC methods, an algorithm is implemented for eliminating the *x-y* stator flux.

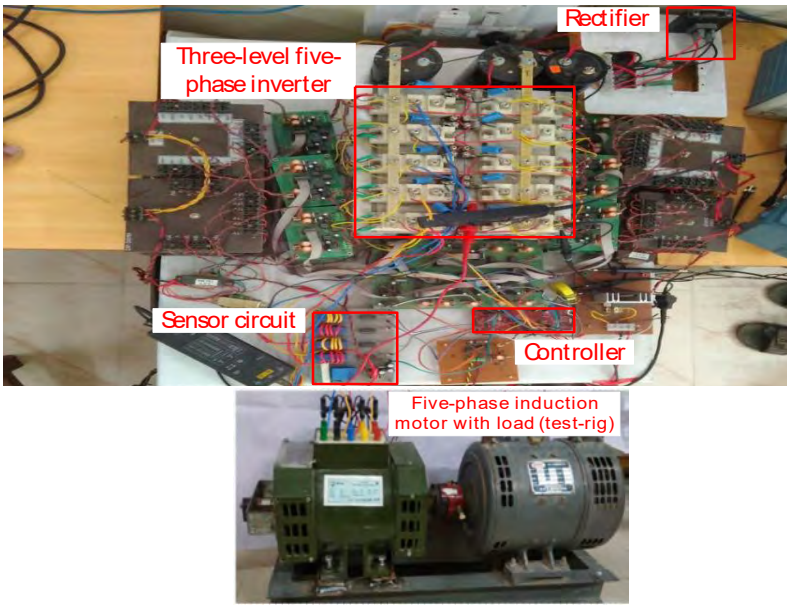

Fig. 6 Experimental set-up of the DTC-II method

Figs. 9 and 10 show the results of dynamic operation wherein rotor speed is increased from zero rpm to 600 rpm. In DTC-I, the *d-q* stator flux starts increasing as the rotor speed increases, however in the DTC-II scheme the *d-q* stator flux maintains its rated value at zero speed and remains at the rated value as the speed increases. The torque ripple in the DTC-II scheme is slightly increased as compared to DTC-I method since the zero voltage vectors are omitted.

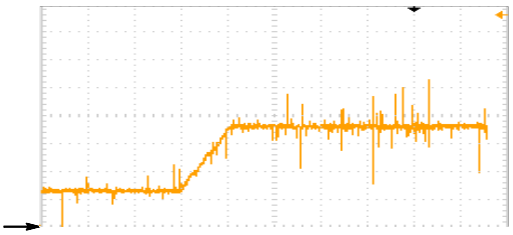

(a)

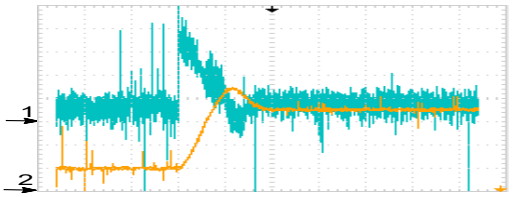

(b)

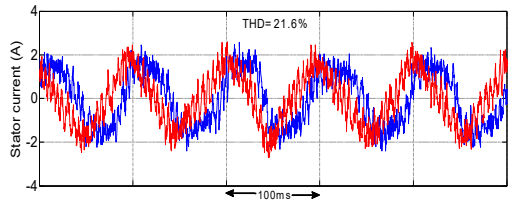

(c)

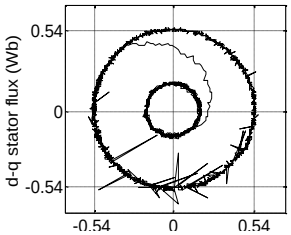

(d)

Fig. 7 Dynamic performance under step change in speed with the DTC-I method, (a) *d-q* stator flux (0.15 Wb/div., 200ms/div.), (b) CH.1 torque (3Nm/div., 200ms/div.), CH. 2 rotor speed (200rpm/div., 200ms/div.), (c) stator current and (d) trajectory of *d-q* stator flux.

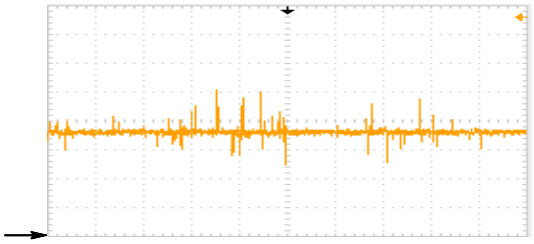

(a)

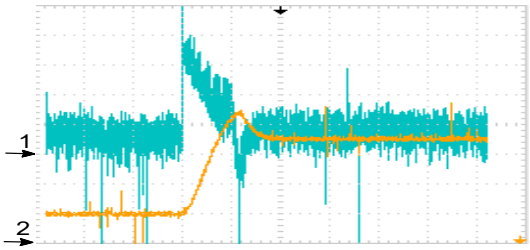

(b)

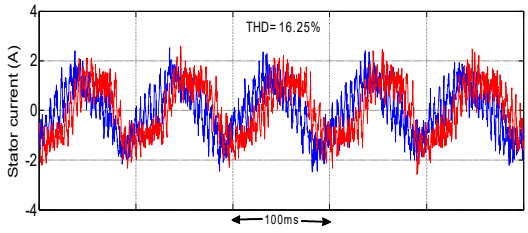

(c)

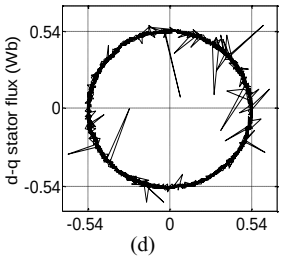

(d)

Fig. 8 Dynamic performance under step change in the speed with the DTC-II method, (a) *d-q* stator flux (0.15 Wb/div., 200ms/div.), (b) CH.1 torque (3Nm/div., 200ms/div.), CH. 2 rotor speed (200rpm/div., 200ms/div.), (c) stator current and (d) trajectory of *d-q* stator flux.

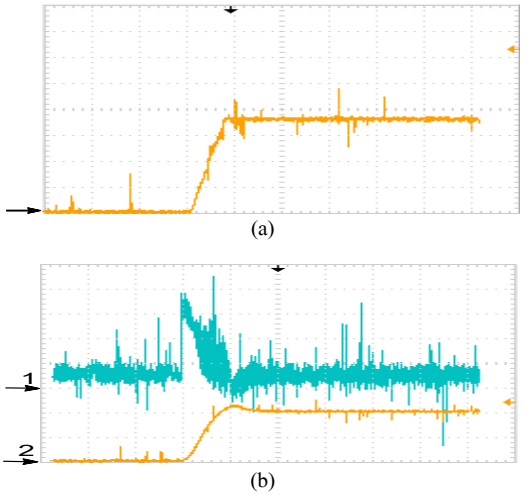

(a)

(b)

Fig. 9 Dynamic performance under step change in speed from zero with DTC-I method, (a) *d-q* stator flux (0.15 Wb/div., 200ms/div.) and (b) CH.1 torque (4Nm/div., 200ms/div.), CH. 2 rotor speed (300rpm/div., 200ms/div.).

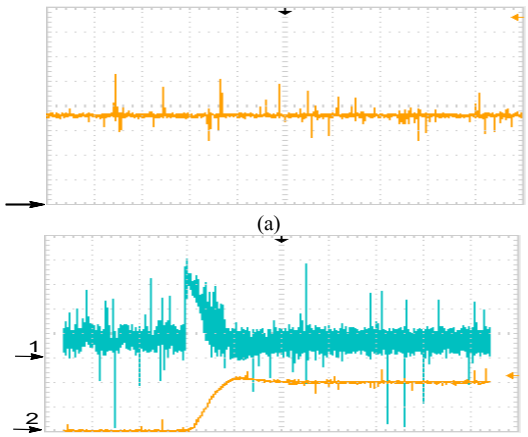

(a)

(b)

Fig. 10 Dynamic performance under step change in speed from zero with DTC-II method, (a) *d-q* stator flux (0.15 Wb/div., 200ms/div.) and (b) CH.1 torque (4Nm/div., 200ms/div.), CH. 2 rotor speed (300rpm/div., 200ms/div.).

Fig. 11 shows the operation of DTC-I and DTC-II schemes when they are operated above low speed range. Once the DTC-II scheme enters into the normal speed region the four level torque comparator is replaced by the seven-level torque comparator that reduces the torque ripple compared to DTC-I. Fig. 12 shows the torque ripple in both the DTC schemes with varying speed command. It is observed that under low speed region (below 20 % of the rated speed) the torque ripple of the DTC-II scheme is higher than the DTC-I scheme. Once the rotor speed comes under normal speed range seven-level torque comparator starts working in DTC-II method and hence torque ripple gets reduced compared to DTC-I method [16]. Fig. 13 shows variation of average switching frequency with respect to variation in speed. Under low speed region, average switching frequency in DTC-I is higher than in DTC-II because in DTC-I five-level torque comparator is implemented and in DTC-II four level torque comparator is implemented. Once the speed enters into the normal speed region (beyond 20% of the rated speed), in DTC-II seven-level torque comparator comes into action and average switching frequency increases compared to DTC-I [16].

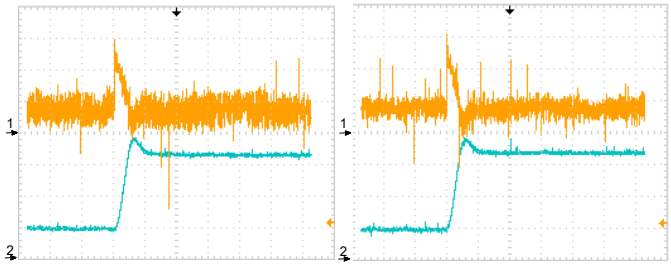

(a) (b)

Fig. 11 Dynamic operation under step change in rotor speed, (a) DTC-I and (b) DTC-II (CH. 1 torque, 3Nm/div., 400ms/div., CH. 2 speed, 300rpm/div., 400ms/div).

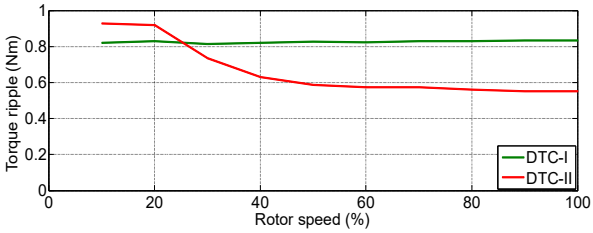

Fig. 12 Torque ripple with respect to rotor speed in both the DTC schemes.

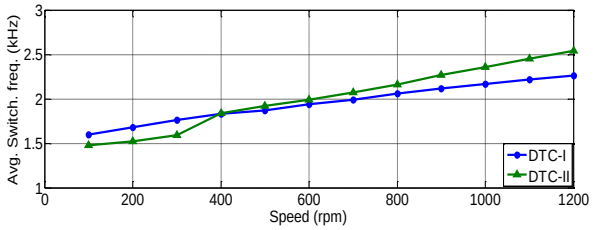

Fig. 13 Average switching frequency with respect to rotor speed in both the DTC schemes.

VI. Conclusion

The DTC technique for five-phase induction motor fed from three-level five-phase inverter is proposed to minimize the demagnetization effect during low speed operation. In order to minimize the demagnetization effect, the 60 main and intermediate voltage vectors among available 243 are selected to design the DTC strategy. In the proposed DTC-II method zero voltage vectors are omitted. This scheme retains the feature of classical DTC strategy, i.e. the simplicity of control algorithm. The torque ripple is also controlled through seven-level torque comparator. The *x-y* stator flux has been eliminated in DTC-II method. From the results it is concluded

that the DTC-II has successfully minimized the demagnetization effect in the low speed region.

VII. References

[1] I. Takahashi and T. Noguchi, بA new quick response and high efficiency control strategy of an induction motor,پ*IEEE Trans. on Ind. Appl.*, vol. 22, no. 5, pp. 820ت827, Sep. 1986.

[2] H. Xu, H. Toliyat, and L. Petersen, بFive-phase induction motor drives with dsp-based control system,پ*IEEE Trans. on Power Electron.*, vol. 17, no. 4, pp. 524ت533, Jul 2002.

[3] B. L. Zheng, J. E. Fletcher and X. He, بA novel direct torque control scheme for a sensorless five-phase induction motor drive,پ*IEEE Trans. Ind. Electron.*, vol. 58, no. 2, pp. 503ت513, Feb 2011.

[4] Shuai Lu, K. Corzine, بDirect torque control of five-phase induction motor using space vector modulation with harmonics elimination and optimal switching sequence,پAPEC ف06, 2006.

[5] L. Gao, J. Fletcher, and L. Zheng, بLow-speed control improvements for a two-level five-phase inverter-fed induction machine using classic direct torque control,پ*IEEE Trans. Ind. Electron.*, vol. 58, no. 7, pp. 2744ت 2754, July 2011.

[6] S. Payami; R. K. Behera, "An Improved DTC Technique for Low Speed Operation of a Five-Phase Induction Motor," in *IEEE Transactions on Industrial Electronics* , vol.PP, no.99, pp.1-1.

[7] K. B. Lee, J. H. Song, I. Choy and J. Y. Yoo, بImprovement of low speed operation performance of DTC for three-level inverter fed induction motors,پ*IEEE Trans. Ind. Electron*., vol. 48, no. 5, pp. 255ت264, Oct. 2001.

[8] I. M. Alsofyani and N. R. N. Idris, "Simple Flux Regulation for Improving State Estimation at Very Low and Zero Speed of a Speed Sensorless Direct Torque Control of an Induction Motor," in *IEEE Transactions on Power Electronics*, vol. 31, no. 4, pp. 3027-3035, April 2016.

[9] I. M. Alsofyani and N. R. N. Idris, "Lookup-Table-Based DTC of Induction Machines With Improved Flux Regulation and Extended Kalman Filter State Estimator at Low-Speed Operation," in *IEEE Transactions on Industrial Informatics*, vol. 12, no. 4, pp. 1412-1425, Aug. 2016.

[10] L. Gao and J. E. Fletcher, بA space vector switching strategy for Three-level five-phase inverter drives,پ*IEEE Trans. on Ind. Electron.*, vol. 57, no. 7, p. 23322343, July 2010.

[11] F. Y. Q. Song, X. Zhang and C. Zhang, بResearch on space vector pwm of five-phase three-level inverter,پ*in Proc. 8th ICEMS*, vol. 2, pp. 1418 ت 1421, Sep. 2005.

[12] Y. N. Tatte and M. V. Aware, "Torque ripple minimization in five-phase three-level inverter fed direct torque control induction motor drive," *Power Electronics and Applications (EPE'15 ECCE-Europe), 2015 17th European Conference on*, Geneva, 2015, pp. 1-6.

[13] Y. Tatte; M. Aware, "Direct Torque Control of Five-Phase Induction Motor with Common-Mode Voltage and Current Harmonics Reduction," in *IEEE Transactions on Power Electronics* , vol. PP, no. 99, pp. 1-1.

[14] Yuan Ren; Zhu, Z. Q., "Reduction of Both Harmonic Current and Torque Ripple for Dual Three - Phase Permanent - Magnet Synchronous Machine Using Modified Switching ت Table - Based Direct Torque Control, "in *Industrial Electronics, IEEE Transactions on*, vol. 62, no. 11, pp. 6671-6683, Nov. 2015.

[15] Yogesh N. Tatte, Mohan V. Aware, Jay K. Pandit, Ronak Nemade, بPerformance Improvement of Three-Level Five-Phase Inverter Fed DTC Controlled Five-Phase Induction Motor during Low-Speed Operationپ PEDES, Kerala, India, 2016.

[16] Y. Tatte; M. Aware, بTorque Ripple and Harmonic Current Reduction in Three-Level Inverter Fed Direct Torque Controlled Five-Phase Induction Motorپ *IEEE Transactions on Industrial Electronics*, vol. PP, no. 99, pp. 1-1.

[17] Y. Zhang, J. Zhu, Z. Zhao, W. Xu and D. G. Dorrell, "An Improved Direct Torque Control for Three-Level Inverter-Fed Induction Motor Sensorless Drive," in *IEEE Transactions on Power Electronics*, vol. 27, no. 3, pp. 1502-1513, March 2012.

[18] S. Payami; R. Kumar Behera; A. Iqbal, "DTC of Three-Level NPC Inverter fed Five-Phase Induction Motor Drive with Novel Neutral Point Voltage Balancing Scheme," in *IEEE Transactions on Power Electronics* , vol. PP, no.99, pp.1-1.